การสังเคราะห์ $LiZnPO_4$ อย่างง่ายโดยผ่านการเปลี่ยนแปลงเชิงความร้อนของ α-$LiZnPO_4{\cdot}H_2O$ –การศึกษาสเปกโทรสโกปีอินฟราเรดและรามาน

A Facile Synthesis of $LiZnPO_4$ via thermal transformation of α -$LiZnPO_4$ H_2O - IR and Raman spectroscopic studies

Nantawat Phonchan[1], Pittayagorn Noisong[1,*], Chanaiporn Danvirutai[1] and Sujittra Youngme[1]

[1]Materials Chemistry Research Center, Department of Chemistry, and Center of Excellence for Innovation in Chemistry (PERCH-CIC), Faculty of Science, Khon Kaen University, Khon Kaen 40002, Thailand

[*]Corresponding Author, E-mail: pittayagorn@kku.ac.th

Received: 30 April 2019 | Revised: 9 July 2019 | Accepted: 7 August 2019

บทคัดย่อ

ได้สังเคราะห์ α-$LiZnPO_4{\cdot}H_2O$ และ สารที่เจือจางด้วยไอโซโทปดิวทีเรียม ด้วยวิธีอย่างง่ายจากสารละลายในน้ำ ณ อุณหภูมิห้อง และผลิตภัณฑ์เชิงความร้อน $LiZnPO_4$ สามารถทำได้ที่อุณหภูมิต่ำ สามารถพิสูจน์เอกลักษณ์ด้านสูตรเคมีและโครงสร้างผลึกด้วยวิธี TG DSC XRD FTIR และ FT Raman ได้รายงานสเปกตรัมเอฟทีอินฟราเรดและเอฟทีรามานของสารที่เจือจางด้วยไอโซโทปดิวทีเรียมพร้อมทั้งศึกษาพฤติกรรมการสั่น ได้อภิปรายความสัมพันธ์ระหว่างการศึกษาเอฟทีอินฟราเรดและเอฟทีรามานสเปกโทรสโกปีกับการวิเคราะห์การแยกสนามสหสัมพันธ์ (correlation field splitting analysis) พบว่า การแยกสนามสหสัมพันธ์ของ H_2O และ HOD ในสารประกอบ α-$LiZnPO_4{\cdot}H_2O$ ได้นำเสนอว่ามีสัญลักษณ์เป็น C_{2v}–C_1–$C_{2v}{}^9$ และ C_s–C_1–$C_{2v}{}^9$ ตามลำดับ ซึ่งรูปแบบการสั่นของทั้งสองสปีชีส์คือ $\Gamma_{Vib} = 3A_1 + 3A_2 + 3B_1 + 3B_2$ ดังนั้น จำนวนแบบการสั่นที่ให้สเปกตรัมอินฟราเรดเป็น 27 แบบ และสำหรับรามานเป็น 36 แบบ ส่วนในกรณีของ $PO_4{}^{3-}$ จะปรากฏแบบการสั่นที่ให้สเปกตรัมอินฟราเรดนั้นเป็น 18 แบบ [$6A_1 + 6B_1 + 6B_2$] และสำหรับรามานนั้นเป็น 36 แบบ [$9A_1 + 9A_2 + 9B_1 + 9B_2$] ได้คำนวณค่าระยะห่างระหว่างอะตอมออกซิเจน ($R_{O\cdots O}$) และเอนทาลปีของการเกิดพันธะไฮโดรเจน (ΔH_H) ของไฮเดรตที่ศึกษาโดยอาศัยข้อมูลทางสเปกโทรสโกปีอีกด้วย

ABSTRACT

The α-$LiZnPO_4{\cdot}H_2O$ was synthesized via a facile synthesis in an aqueous solution at ambient temperature. Its deuterated analogue was synthesized using the same manner and the calcined product $LiZnPO_4$ was obtained at low heating temperature. The chemical formula and crystal structure of α-$LiZnPO_4{\cdot}H_2O$ and its calcined product were characterized by using TG, DSC, XRD, FTIR and FT Raman methods. The FTIR/FT Raman spectra of the deuterated analogue were reported in this work and the vibrational behaviors of all samples were studied. The relation between FTIR/FT Raman spectroscopic study and the correlation field splitting analysis are discussed. The correlation field splitting analysis of H_2O and HOD molecules in α-$LiZnPO_4{\cdot}H_2O$ are symbolized as C_{2v}–C_1–$C_{2v}{}^9$ and

C_s–C_1–C_{2v}[9], respectively, which suggested the number of vibrational modes to be: Γ_{Vib} = $3A_1$ + $3A_2$ + $3B_1$ + $3B_2$ for both species. Thus, the 27 internal vibrational modes are infrared active and 36 are Raman active. In the case of PO_4^{3-}, It exhibits 18 IR [$6A_1$ + $6B_1$ + $6B_2$] and 36 Raman [$9A_1$ + $9A_2$ + $9B_1$ + $9B_2$] active bands. The distance between oxygen atoms ($R_{O\cdots O}$) and the enthalpy of hydrogen bonding (ΔH_H) of the studied hydrate were estimated from the spectroscopic data.

คำสำคัญ: α-$LiZnPO_4{\cdot}H_2O$ เอฟทีอินฟราเรด เอฟทีรามาน ระเบียบวิธีการสหสัมพันธ์

Keywords: α-$LiZnPO_4{\cdot}H_2O$, FTIR, FT Raman, Correlation Method

INTRODUCTION

The binary metal orthophosphates of the type $M^{I}M^{II}PO_4{\cdot}H_2O$ and their calcined product can form a widely family of compounds. The anhydrous type of M^{I} = Li^+ and M^{II} = Fe^{2+}, Mn^{2+}, Co^{2+} and Ni^{2+} with an olivine structure have attracted considerable attention as cathode materials for rechargeable lithium-ion batteries (Liu et al., 2011; Fan et al., 2016, Ma et al., 2017). The materials are excellent for their cycle ability, thermal stability, low-cost, and environmental friendliness (Fan et al., 2016; Xu et al., 2018). The compounds $LiZnPO_4{\cdot}H_2O$, $LiZnPO_4$, $NaCoPO_4$, $KCoPO_4$ and NH_4CoPO_4 have attracted great interest in the last two decades because of their potential to form framework structures similar to aluminosilicate zeolite (Feng et al., 1997; Jensen, 1998; Liao et al., 2009). The potential applications of some framework phosphates are for examples as sorption of metal ions (Mustafa et al., 2005), adsorption of small molecules (Ismailova et al., 1996) and catalysts (Li et al., 2009). The hydrate form of $LiZnPO_4{\cdot}H_2O$ was described as having a zeolite type ABW structure, *i.e.* isomorphous with zeolite Li-ABW, $LiAlSiO_4{\cdot}H_2O$ (Jensen, 1998; Harrison et al., 1995; Liao et al., 2009). In addition, the anhydrous $LiZnPO_4$ was reported to be the host for Mn^{2+} doped in potential applications as a phosphor in LEDs and can be expected to be a novel green-yellow emitting phosphor for light emitting diode (Chan et al., 2008; Chan et al., 2008). The preparations of the $LiZnPO_4{\cdot}H_2O$ have been reported at both high (hydrothermal method) (Harrison et al., 1995; Jensen, 1998) and low temperatures (Liao et al., 1995). For example, Jensen (1998) has reported various synthetic routes for this compound. Harrison et al. (1995) reported the synthesis of $LiZnPO_4{\cdot}H_2O$ by using hydrothermal method at 70 °C for 1–2 days. According to the mentioned works, the α-$LiZnPO_4{\cdot}H_2O$ which belongs to the *Pna2₁* or C_{2v}^9 space group, having an orthorhombic crystal structure, and containing four molecules per unit cell (Z = 4), a = 10.575(2) Å, b = 8.0759(6) Å, c = 4.9937 Å and V = 426.5 $Å^3$. Liao et al. (2009) presented that the crystallinity and thermal properties of α-$LiZnPO_4{\cdot}H_2O$ depend on the synthetic routes. The synthesis of $LiZnPO_4{\cdot}H_2O$ has been extensively studied, unfortunately, those synthetic routes were time consuming and difficult (Jensen, 1998; Harrison et al., 1995; Liao et al., 2009; Chen et al., 2012).

Vibrational spectroscopic study has a potential for providing the information of about the crystalline phase transition such as α-$LiZnPO_4{\cdot}H_2O$ to $LiZnPO_4$ (Dhevi et al., 2018), investigation of crystal structure (Ansari and Majeed Khan, 2018), quantification purpose (Adichtchev and Surovtsev, 2018), characterization or diagnosis of healthy and dengue infected human blood plasma sample (Mahmood et al., 2018). There are some information about the vibrational spectroscopic study of the phosphate minerals (Frost et al., 2006; Frost and

Xi, 2012; Frost et al., 2013). Infrared and Raman spectra of magnesium ammonium phosphate hexahydrate $MgNH_4PO_4 \cdot 6H_2O$ or the synthetic struvite and its isomorphous analogues have been studied by Stefov et al. (2004; 2005; 2008; 2009; 2013), Šoptrajanov et al. (2004; 2011) and Cahil et al. (2007; 2008). The H-O-H bending was generally observed at about 1600 cm^{-1}, however the very low H-O-H bending (at about 1400 cm^{-1}) of some metal phosphate hydrates were found by Šoptrajanov (2000), Pejov et al. (2000) and Šoptrajanov et al. (2002). However, the details of vibrational spectroscopic study of the title compound have been slightly presented (Jensen, 1998; Liao et al., 2009). Consequently, the estimation of the distance between the oxygen atoms of two H-bonding water molecules (H_2O, HOD, D_2O). In this study, the system was HOD(D_2O). as well as the enthalpy of hydrogen bond (ΔH_H) were less studied (Badger and Bauer, 1937; Rao et al., 1975; Luck, 1976; Buanam- Om, 1981; Danvirutai and Jeladipalang, 1984). Therefore, the development of synthetic method with better condition and the vibrational spectroscopy of α- $LiZnPO_4 \cdot H_2O$ and its deuterated analogue are of considerable interest in this work as the study of synthesis and vibrational spectroscopy of some metal phosphates (Kullayakool et al., 2013; Sronsri et al., 2016) and manganese hypophosphite monohydrate (Noisong and Danvirutai 2010) in our previous work.

The purposes of this work are to present the facile synthesis of α-$LiZnPO_4 \cdot H_2O$ which is cost effective and environmental benign compared with that report in the literatures and to report the vibrational spectroscopic study results using Fourier transform infrared (FTIR) and Fourier transform Raman (FT Raman) techniques. The synthesized α- $LiZnPO_4 \cdot H_2O$ samples were characterized by X-ray powder diffraction (XRD), thermogravimetry/ differential thermogravimetry/ differential thermal analysis (TG/DTG/DTA), gravimetric analysis, Karl Fischer (KF), and atomic absorption/atomic emission spectrophotometry (AAS/AES). The FTIR and FT Raman spectra of the hydrate, its deuterated analogue and its calcined product were compared. The vibrational band positions can be assigned and discussed based on the vibrational energy values of H_2O, D_2O, HOD and phosphate (PO_4^{3-}) species. In general, the combination of vibrational and group theory studies is important in solving problems of molecular structure as well as determination or confirmation of molecular structure, Thus, the correlation method or factor group analysis was investigated and consistently discussed with the FTIR/ FT Raman spectra. In addition, the distance between oxygen and oxygen ($R_{O\cdots O}$) as well as the enthalpy of hydrogen bond (ΔH_H) were estimated.

RESEARCH METHODOLOGY

Preparations and characterizations

The α- $LiZnPO_4 \cdot H_2O$ samples were synthesized by using the ratio Li: Zn: P of 3: 1: 1 applied from the synthesis of $LM^{II}PO_4$ cathode materials (M^{II} = Mn, Fe, Co, Ni) (Chen et al., 2008). In a typical synthesis, 0.69 g (accurate 5.00 mmol) of $ZnCl_2$ (Carlo Erba) was dissolved in 5.00 mL of 1.00 M H_3PO_4 (5.00 mmol, Carlo Erba) and stirred until a clear solution was obtained. Then 0.63 g of $LiOH \cdot H_2O$ (Fluka) was dissolved in about 10 mL of de-ionized (DI) water and stirred until it was completely dissolved. Then, the mixture solution of $ZnCl_2$ and H_3PO_4 was added dropwise by the solution of $LiOH \cdot H_2O$. A milky suspension was stirred constantly at room temperature for about 15 min. The white solid was filtered by a suction pump, washed several times with DI water to prepare α- $LiZnPO_4 \cdot H_2O$ and kept in a desiccator for overnight to prevent the moisture. The deuterated analogue samples were synthesized in a

same manner as mentioned above by using LiOH ($LiOH{\cdot}H_2O$ calcined at 120 °C (Kim et al., 2000) and D_3PO_4 substitute for $LiOH{\cdot}H_2O$ and H_3PO_4, respectively. The as-prepared product was calcined at 250 °C for 2 h and its final decomposition product was confirmed to be $LiZnPO_4$.

The structures of the prepared sample and its calcined product were characterized by X-ray powder diffraction (XRD) using a powder diffractometer (Philips PW3710) with a $CuK\alpha$ radiation (λ = 1.5406 nm). The diffraction patterns were taken at $10° < 2\theta < 60°$ with 0.02° step size. Thermal property of the synthesized α-$LiZnPO_4{\cdot}H_2O$ was investigated using thermogravimetry/ differential thermogravimetry/ differential thermal analysis (TG/ DTG/ DTA, Perkin Elmer Pyris Diamond). The TG/DTG/DTA measurement was carried out using about 5 mg (accurate) mass of the powder sample filling in an open alumina pan. The TG/DTG/DTA curves were recorded over the temperature range of 50–400 °C at the heating rate of 10 K min^{-1} in N_2 atmosphere with the flow rate of 100 mL min^{-1} using α-Al_2O_3 as the standard reference material. The water content was determined by using gravimetric analysis, TG/DTG/DTA and Karl Fischer techniques. Zinc and lithium contents were determined using atomic absorption spectrophotometry (AAS) and atomic emission spectrophotometry (AES), respectively, by dissolving the hydrate sample in the diluted nitric acid (Perkin Elmer Analyst 100).

Studies of FTIR/ FT Raman spectroscopy and correlation field splitting analysis

The FTIR spectra of the hydrate sample, its deuterated analogue and its calcined product were recorded over the wavenumber range of 4000 to 370 cm^{-1} using KBr pellet technique (KBr, Merck, Spectroscopy grade) on a Perkin Elmer spectrum GX FTIR/FT Raman spectrophotometer with 16 scans and the resolution of 4 cm^{-1}. Their FT Raman spectra were recorded on the same instrument over the Raman shift range of 4000 to 100 cm^{-1} with 32 scans and the resolution of 4 cm^{-1}.

The correlation field splitting or factor group analysis was studied by taking only the vibrational symmetry species into account. The number of IR active and Raman active modes of vibrations can be derived from the irreducible representations for; (i) the point group symmetry of free ion or molecule, (ii) the site group symmetry and (iii) the unit cell group which is isomorphous with the factor group (Falk and Khop, 1973). The discussion between the results analyzed from correlation field splitting analysis and the band positions appearing in FTIR/FT Raman can be carried out.

Estimation of $R_{O\cdots O}$ and ΔH_H from ν_{OH}(HOD) or ν_{OD}(HOD)

The correlation between $R_{O\cdots O}$ and ν_{OH} or ν_{OD} of the single or uncoupled OH or OD oscillator were described by Buanam-Om (1981) as expressed in Eqs. (1) to (4), respectively.

$$R_{O\cdots O} = 4.105\ (Å) - 0.2201(Å)\ \ln(\Delta\nu_{OH}/cm^{-1}) \quad (1)$$

$$\Delta\nu_{OH} = 3707 - \nu_{OH,\,obs}(HOD)\ cm^{-1} \quad (2)$$

$$R_{O\cdots O} = 4.120\ (Å) - 0.2371(Å)\ \ln(\Delta\nu_{OD}/cm^{-1}) \quad (3)$$

$$\Delta\nu_{OD} = 2727 - \nu_{OD,\,obs}(HOD)\ cm^{-1} \quad (4)$$

Direct proportionality between frequency shift ($\Delta\nu$) and H-bond energy becomes a conventional assumption in the H-bond spectroscopy (Luck, 1976). The first experimental indication for $\Delta\nu \propto \Delta H$ was given by Badger and Bauer (1937). Reexamination of the so-called Badger-Bauer's rule was carried out by Rao et al. (1975). Theoretical aspects of this rule were treated by Purcell and Drago (1967). So far, the relation, $\Delta\nu \propto \Delta H$ is true only for the same homologous series.

General linear relation, $\Delta\nu = a\,\Delta H + b$ was found (Rao et al., 1975; Luck, 1976).

The deuterated analogues of hydrates have been studied by using IR and Raman spectroscopy by observing the uncoupled ν_{OH}(HOD) in both techniques. The uncoupled ν_{OH}(HOD) values lead to the estimation of ΔH_H (kJ mol^{-1} OH) from following equation which has been presented by Buanam-Om (1981) as well as Danvirutai and Jeradipalan (1984).

$$-\Delta H_H = 1.286 + 0.0418\,(\Delta\nu_{OH}(HOD)/cm^{-1}) \qquad (5)$$

RESULTS AND DISCUSSION

TG/DTG/DTA

The TG/DTG/DTA thermograms of the prepared α-$LiZnPO_4{\cdot}H_2O$ are shown in Figure 1. The observed mass loss at the heating rate of 10 K min^{-1} in N_2 atmosphere is 9.35% corresponds to the mass loss of water molecules. The dehydration was observed as a single stage over the temperature range of 50–400 °C. The DTA peak agrees with the DTG peak at 169.9 °C. The dehydration reaction is suggested to be as following:

$$\alpha\text{-}LiZnPO_4{\cdot}H_2O(s) \longrightarrow LiZnPO_4(s) + H_2O(g) \qquad (6)$$

The water molecules in the crystal structure can be classified into two types: the first one is water of crystallization which the elimination of water occurs at 150 °C and below, whereas the last one was eliminated at around 150 and less than 200 °C, which indicated the water coordinately linked with metal cation (Feng et al., 1997).

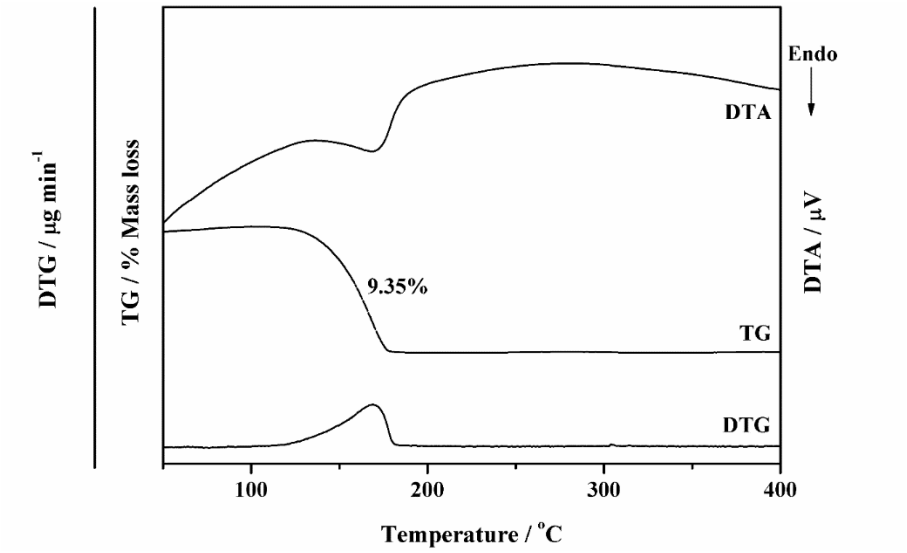

Figure 1 TG/ DTG/ DTA thermograms of the prepared α-$LiZnPO_4{\cdot}H_2O$ at a heating rate of 10 K min^{-1} in N_2 atmosphere

XRD and chemical formula

The XRD patterns of the prepared α-$LiZnPO_4{\cdot}H_2O$ and its calcined product at 250 °C in N_2 atmosphere are shown in Figure 2. The detectable peaks of the prepared sample and the calcined product are indexed as the structure of α-$LiZnPO_4{\cdot}H_2O$ (a) and its thermal dehydration product $LiZnPO_4$ (b) according to the standard ICDD card No. 01-083-0263 (orthorhombic, space group $Pna2_1$ or C_{2V}^9, Z = 4) and ICDD card No. 01-083-0264 (orthorhombic, space group $Pn2_1a$), respectively. The lattice parameters of the prepared α-$LiZnPO_4{\cdot}H_2O$ calculated from XRD patterns are found to be a = 10.384 Å, b = 8.0872 Å and c = 4.9938 Å. While, those of its calcined product $LiZnPO_4$

are found to be a = 10.02 Å, b = 6.653 Å and c = 4.971 Å. These values are agreeing very well with the reported standard data (Harrison et al., 1995).

The water contents determined from TG thermogram at a heating of 10 K min^{-1} and gravimetric analysis were found to be 0.96 and 1.01 mol per formula, respectively. Water content determined from Karl Fischer (KF) technique was found to be 0.97 mol. The lithium and zinc contents determined from AES and AAS, were found to be 1.04 and 0.99 mol per formula, respectively. According to TG/ DTG/ DTA, gravimetric analysis, KF technique, AAS and AES, and XRD results, the chemical formula of the as-prepared sample was confirmed to be α-$LiZnPO_4 \cdot H_2O$.

The complete dehydration of the α-$LiZnPO_4 \cdot H_2O$ in N_2 atmosphere was obtained by heating in the furnace at 250 °C for 2 h and the final transformation product was found to be $LiZnPO_4$ as confirmed by using the mentioned above techniques. The thermal transformation of α-$LiZnPO_4 \cdot H_2O$ is found to be the single dehydration process. Consequently, the synthetic route of α-$LiZnPO_4 \cdot H_2O$ is relatively simple, compared with those reported in the literatures (Harrison et al., 1995; Feng et al., 1997; Jensen, 1998, Liao et al., 2009).

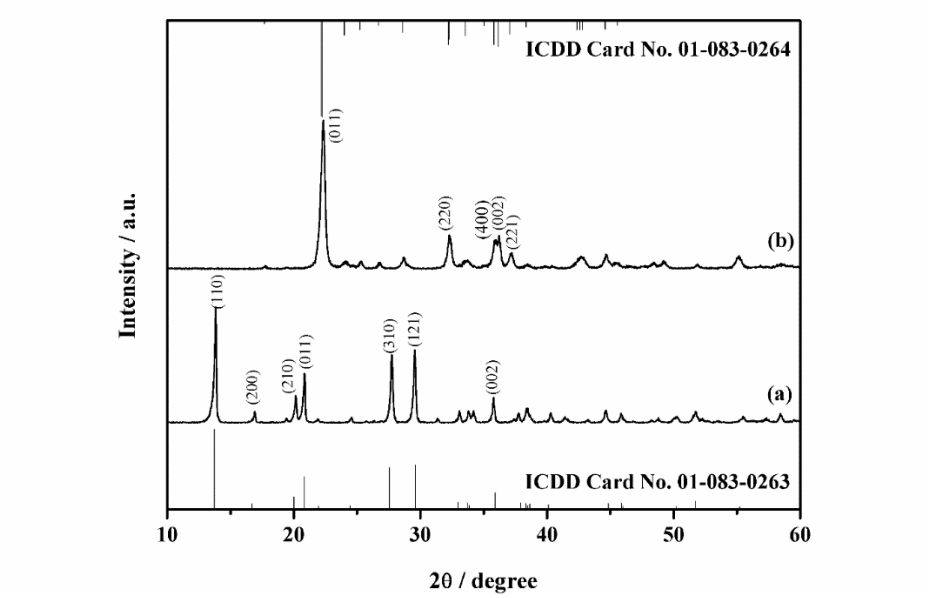

Figure 2 XRD patterns of the prepared α-$LiZnPO_4 \cdot H_2O$ (a) and its calcined product at 250 °C, $LiZnPO_4$ (b)

FTIR/FT Raman spectroscopy

The FTIR spectra of the prepared sample, its deuterated analogue and its calcined product in the wavenumber range of 4000–370 cm^{-1} are presented in Figure 3. The FTIR spectrum of α-$LiZnPO_4 \cdot H_2O$ illustrated in Figure 3a is similar to that reported by Jensen (1998). The free H_2O molecule possessing C_{2V} symmetry has three normal vibrational modes, namely symmetric stretching $\nu_1(A_1)$, the asymmetric stretching $\nu_3(B_2)$ and the bending $\nu_2(A_1)$ vibrations. The bands at 3594 and 3487 cm^{-1} are assigned to $\nu_3(B_2)$ and $\nu_1(A_1)$ of H_2O, respectively. The band at 1609 cm^{-1} is assigned to $\nu_2(A_1)$ of H_2O. Two bands at 671 and 471 cm^{-1} are assigned to the librational modes $\rho_r(H_2O)$ and $\rho_w(H_2O)$, respectively, for their disappearance in the FTIR spectrum of the calcined product as shown in Figure 3c. In Figure 3b, the bands at 2668, 2527 and 1188 cm^{-1} are assigned to $\nu_3(B_2)$, $\nu_1(A_1)$ and $\nu_2(A_1)$ of D_2O molecules, while the bands at 3569 and 2571 cm^{-1} are assigned to ν_{OH}(HOD) and ν_{OD}(HOD), respectively. The vibrational

bands of D_2O and HOD can be assigned by based on the difference between FTIR spectrum of the α-$LiZnPO_4{\cdot}H_2O$ in Figure 3a and its deuterated analogue in Figure 3b. The bands at 1123, 1083, 1064, 1038 and 1009 cm^{-1} assigned to the asymmetric stretching $\mathbf{V}_3(F_2)$, while one band at 982 cm^{-1} is assigned to the symmetric stretching $\mathbf{V}_1(A_1)$ of PO_4^{3-}. The bands at 630, 616, 576, 563 and 504 cm^{-1} are assigned to the asymmetric bending $\mathbf{V}_4(F_2)$, while two bands at 422 and 415 cm^{-1} are assigned to the symmetric bending $\mathbf{V}_2(E)$ of PO_4^{3-}. The splitting of triply degenerate $\mathbf{V}_3(F_2)$ and $\mathbf{V}_4(F_2)$ as well as the doubly degenerate $\mathbf{V}_2(E)$ bands of PO_4^{3-} vibrating unit indicate the lowering T_d symmetry of the phosphate anion in the crystal structure of the hydrate. The distortion of the structure have been previously reported by Harrison et al. (1995).

The FT Raman spectra of the prepared sample, its deuterated analogue and its calcined product in the Raman shift range of 4000– 100 cm^{-1} are presented in Figure 4. In Figure 4a, two bands appear at 3404 and 3281 cm^{-1} are assigned to $\mathbf{V}_3(B_2)$ and $\mathbf{V}_1(A_1)$ of H_2O, respectively, while two bands at 1620 and 1611 cm^{-1} are assigned to $\mathbf{V}_2(A_1)$ of H_2O. Two bands at 1151 and 1047 cm^{-1} are assigned to $\mathbf{V}_3(F_2)$ PO_4^{3-}, while the band at 991 is assigned to $\mathbf{V}_1(A_1)PO_4^{3-}$. Two bands at 605 and 515 cm^{-1} are assigned to $\mathbf{V}_4(F_2)$ PO_4^{3-}, while the band at 398 cm^{-1} is assigned to $\mathbf{V}_2(E)PO_4^{3-}$. Some vibrational bands were not observed in both FTIR and FT Raman spectra which may be due to the selection rule. The assignment of observed water bands in this study is important for interpreting the interaction between water molecules and their environments. All possible assignments of three samples are summarized in Table 1.

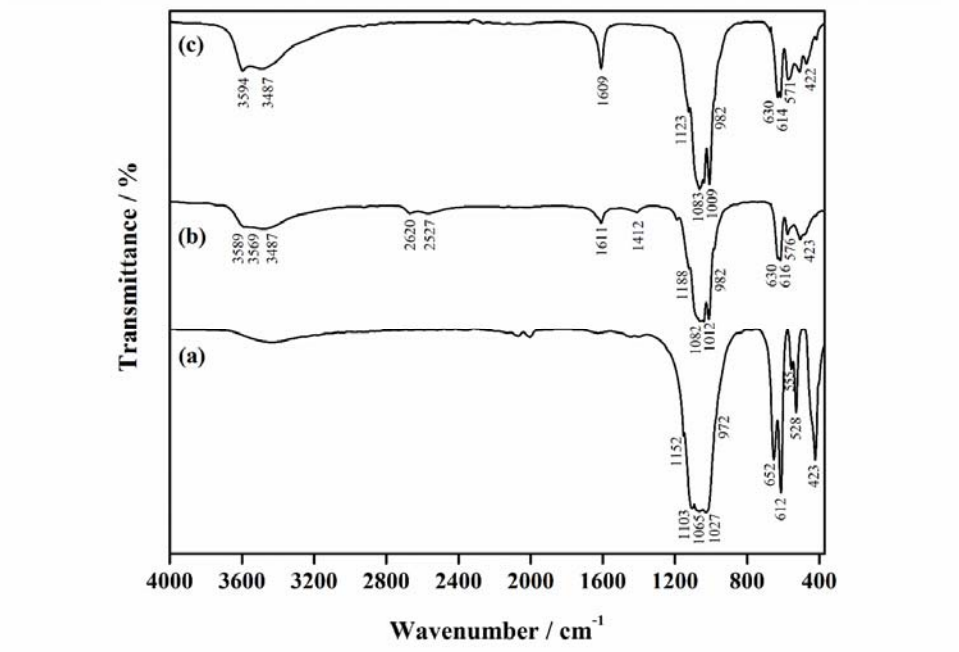

Figure 3 FTIR spectra of calcined product at 250 °C, $LiZnPO_4$ (a), its deuterated analogue (b) and the prepared α-$LiZnPO_4{\cdot}H_2O$ (c) in the wavenumber range of 4000–370 cm^{-1}

Table 1 FTIR/FT Raman band positions and the possible assignments of the prepared α-$LiZnPO_4 \cdot H_2O$, its deuterated analogue and its calcined product at 250 °C $LiZnPO_4$

FTIR bands / cm^{-1}			FT Raman shifts / cm^{-1}			Possible assignments
The prepared	The deuterated	The calcined	The prepared	The deuterated	The calcined	
3594 m	3589 m, b	-	3404 w, b	-	-	$\nu_3(B_2)H_2O$
-	3569 m, sh	-	-	-	-	ν_{OH}(HOD)
3487 m, b	3487 m, sh	-	3281 w, b	3396 w, b	-	$\nu_1(A_1)H_2O$
-	2668 w	-	-	-	-	$\nu_3(B_2)D_2O$
-	2620 w, sh	-	-		-	ν_{OD}(HOD)
-	2571 w, b	-	-	2553 w, sh	-	$\nu_1(A_1)D_2O$
-	2527 w, sh	-	-	2534 w	-	$\nu_1(A_1)D_2O$
-	-	-	1620 w		-	$\nu_2(A_1)H_2O$
1609 m, sp	1611 m, sp	-	1611 w	1617 w	-	$\nu_2(A_1)H_2O$
-	1412 w	-	-	1418 w	-	$\nu_2(A_1)$HOD
-	-	-	-	1355 w	-	$\nu_2(A_1)$HOD
-	1188 w, sh	-	-	-	-	$\nu_2(A_1)D_2O$
-	-	1152 m, sh	1151 m, sp	1149 w	-	$\nu_3(F_2)PO_4^{3-}$
1123 m, sh	1121 m, sh	1103 vs	-	-	1099 w, sp	$\nu_3(F_2)PO_4^{3-}$
1083 vs, sh	1082 vs, sh	-	-	-	-	$\nu_3(F_2)PO_4^{3-}$
1064 vs	1063 vs	1065 vs	-	-	1051 w, sp	$\nu_3(F_2)PO_4^{3-}$
1038 vs	1039 vs	1027 vs	1046 m, sp	1047 w, sp	1024 w	$\nu_3(F_2)PO_4^{3-}$
1009 vs, sp	1012 vs, sp	-	-	-	-	$\nu_3(F_2)PO_4^{3-}$
982 m, sh	982 m, sh	972 m, sh	991 vs, sp	990 vs, sp	987 vs, sp	$\nu_1(A_1)PO_4^{3-}$
671 w, sh	670 w, sh	-	-		-	$\rho_t(H_2O)$
-	-	652 s, sp	-		-	$\nu_4(F_2)PO_4^{3-}$
630 m	630 m	-	-	629 w	-	$\nu_4(F_2)PO_4^{3-}$
614 m	616 m	612 vs, sp	605 w	603 w	618 w	$\nu_4(F_2)PO_4^{3-}$
571 m	576 w	-	-	-	575 w	$\nu_4(F_2)PO_4^{3-}$
-	563 w, sh	555 w, sp	-	-	552 w	$\nu_4(F_2)PO_4^{3-}$
508 w	504 w	528 m, sp	515 v, sp	514 w	-	$\nu_4(F_2)PO_4^{3-}$
471 w	482 w, sh	-	-	-	-	$\rho_r(H_2O)$
-	-	440 m, sh	-	-	431 m, sp	$\nu_2(E)PO_4^{3-}$
422 w, sh	423 w, sh	423 s, sp	-	-	-	$\nu_2(E)PO_4^{3-}$
415 w	417 w, sh	404 w, sh	398 m, sp	-	411 m, sp	$\nu_2(E)PO_4^{3-}$
378 w	375 w, sh	-	-	372 w	378m, sp	ν_{Zn-O}
-	-	-	304 w, sp	-	339 w, sh	ν_{Li-O}
-	-	-	251 w, sh	209 w	218 w, sh	External mode

Note vs = very strong peak; s= strong peak; m = medium peak; w = weak peak; sp = sharp peak and sh = shoulder peak; b = broad peak

Correlation field splitting analysis

This work has presented some approximations for helpful correlating the classification of vibrational modes of molecule or an ion/ species based on molecular point group, site symmetry and space group using correlation method (Halford, 1946; Horning, 1948; Falk and Knop, 1973). The isolated molecule of H_2O and HOD, there are three internal modes as follow: $\Gamma_{Vib} = A_1 + B_1 + B_2$. Since four molecules are present per unit cell ($Z' = 4$) of solid α-$LiZnPO_4{\cdot}H_2O$, and it may be occurred the interaction between the four molecules, the splitting of vibrations can occur which is called correlation field or factor group splitting. It can split that all types of vibrations. Therefore, both H_2O and HOD species in the synthesized compounds, there are 24 external or lattice modes and 12 internal modes. α- $LiZnPO_4{\cdot}H_2O$ and $LiZnPO_4$ crystallize in the orthorhombic system with space group $Pna2_1$ or C_{2v}^9, $Z = Z' = 4$ and the only C_1 site symmetry is possible. Therefore, we may consider both the two molecules lie on a C_1 site (in general, the molecular point group will be of higher order than the site group) the correlation field splitting of H_2O in α- $LiZnPO_4{\cdot}H_2O$ can be symbolized as $C_{2v}-C_1-C_{2v}^9$. While, correlation field splitting of HOD can be symbolized as $C_s-C_1-C_{2v}^9$. The number of modes of both species can be predicted to be $\Gamma_{Vib} = 3A_1 + 3A_2 + 3B_1 + 3B_2$ (Ferraro and Ziomek, 1975). Table 2 illustrates the correlation table for the both H_2O and HOD in a molecular point group C_2v and C_s, respectively, a site group C_1, and the factor group C_{2v}^9. All A and B modes are Raman and infrared active, except for A_2 mode, which is infrared inactive. Thus, for the internal vibration modes 27 are infrared active and 36 are Raman active (for H_2O and HOD molecules).

Correlation field splitting of PO_4^{3-} ion is on a C_1 site in unit cell of both α-$LiZnPO_4{\cdot}H_2O$ and $LiZnPO_4$. The symbol for correlation field splitting of PO_4^{3-} in this case was assigned as $T_d-C_1-C_{2v}^9$ and is shown in Table 3. The PO_4^{3-} should have $(3n-6)Z = [(3\times5)-6]\times4 = 36$ internal modes. The number of internal modes of that species in both compounds can be predicted to be 18 IR [$6A_1 + 6B_1 + 6B_2$] and 36 Raman [$9A_1 + 9A_2 + 9B_1 + 9B_2$] bands. However, the number of internal vibration bands calculated from correlation method are inconsistent with the observed from the spectra because of the occurring of some overlapping peaks.

Estimation of $R_{O\cdots O}$ and ΔH_H from ν_{OH}(HOD) or ν_{OD}(HOD)

The observed ν_{OH}(HOD) and $\Delta\nu_{OH}$(HOD) were used to calculate $R_{O\cdots O}$ and ΔH_H of α-$LiZnPO_4{\cdot}H_2O$. The $R_{O\cdots O}$ distance is the distance between O atom of water molecule and O atom of other water molecule that forms H-bond interaction. The estimation that $R_{O\cdots O}$ can be estimated the strength of occurred H-bonding as the following (Scherer, 1978; Novak, 1974), when the $R_{O\cdots O}$ is lower than about 2.60 Å, in the range of 2.60-2.70 Å and higher than 2.70 Å, it can be demonstrated that the strong, intermediate and week H-bonding, respectively. This work, the $R_{O\cdots O}$ was calculated to be 2.931 Å. This synthesized compound exhibits the weak H-bonding in that structure. The value of ΔH_H was found to be -7.036 kJ mol^{-1}. The calculated enthalpy of hydrogen bonding of α-$LiZnPO_4{\cdot}H_2O$ is reported in this work and shows a weaker hydrogen bond compared with the others binary cation phosphate hydrates in the type $LiM^{II}PO_4{\cdot}nH_2O$ (M^{II} = Mn, Fe, Co and Ni and n = 1–3) reported by Boontima (2010).

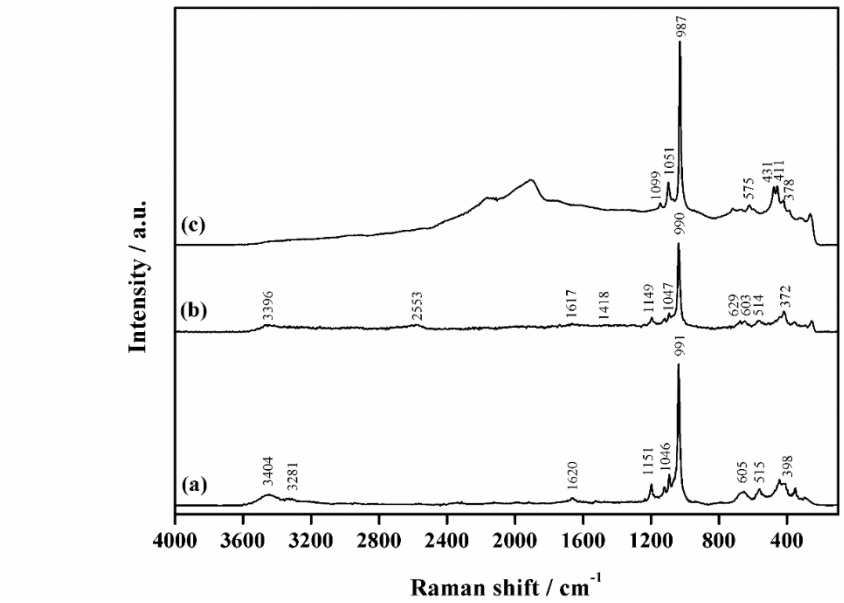

Figure 4 FT Raman spectra of the prepared α-$LiZnPO_4 \cdot H_2O$ (a), its deuterated analogue (b) and its calcined product at 250 °C, $LiZnPO_4$ (c) in the FT Raman shift range of 4000–100 cm^{-1}

Table 2 The correlation table for the internal modes of H_2O (a) and HOD (b) molecules in α-$LiZnPO_4 \cdot H_2O$

(a) Internal vibrations of H_2O molecule

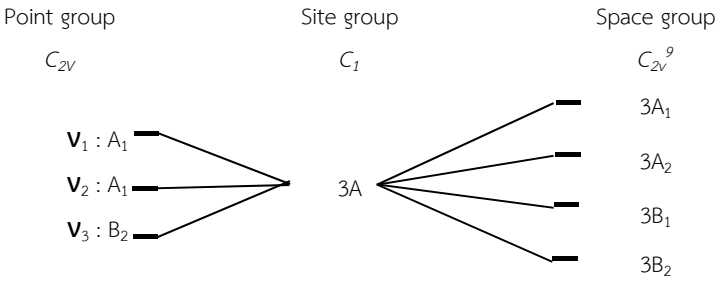

(b) Internal vibrations of HOD molecule

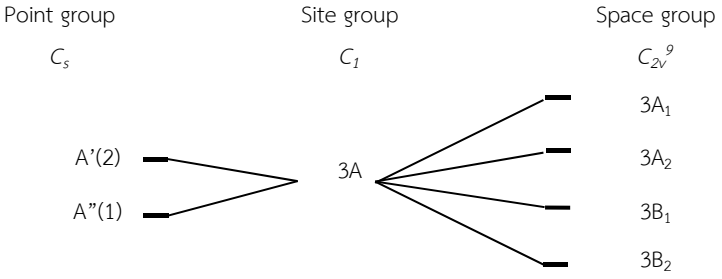

Table 3 Correlation table for the internal modes of PO_4^{3-} anion in α-$LiZnPO_4 \cdot H_2O$

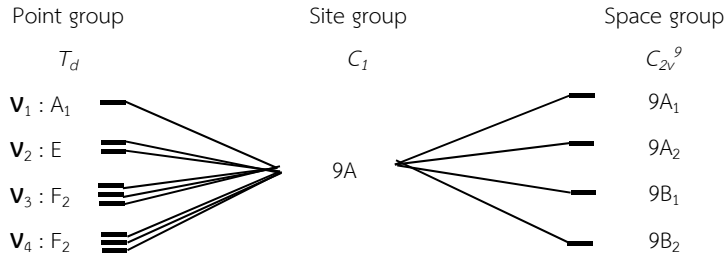

CONCLUSIONS

The α- $LiZnPO_4 \cdot H_2O$ was successfully synthesized by using energy saving and time-consuming method at ambient temperature and pressure. The water content determined from TG data, gravimetric analysis and Karl Fischer method, as well as the lithium and zinc contents determined from AES and AAS, respectively, confirmed the chemical formula. The XRD patterns illustrate the crystal structure of α-$LiZnPO_4 \cdot H_2O$ and its calcined product. The FTIR/ FT Raman spectroscopy was consistently studied in detail for the first time using the deuteration technique and approximation the internal modes of H_2O, HOD molecules and PO_4^{3-} anion in the synthesized compounds by correlation method. The numbers of vibrational bands analyzed from FTIR and FT Raman spectra were found to disagree with those calculated from correlation field analysis. The oxygen- oxygen distance ($R_{O\cdots O}$) of the synthesized compound and hydrogen bond enthalpy (ΔH_H) were found to be 2.931 Å. and –7.036 kJ mol^{-1}, respectively.

ACKNOWLEDGMENTS

We thank the Department of Chemistry and the Department of Physics (for XRD), Faculty of Science, Khon Kaen University for providing research facilities. The financial supports from the Materials Chemistry Research Center, Department of Chemistry, and Center of Excellence for Innovation in Chemistry (PERCH-CIC), Faculty of Science, Khon Kaen University are gratefully acknowledged.

REFERENCES

Adichtchev, S.V. and Surovtsev, N.V. (2018). Raman spectroscopy for quantification of water-to-lipid ratio in phospholipid suspensions. Vib. Spectrosc. 97: 102-105.

Ansari, A. A. and Majeed Khan. M. A. (2018). Structural and spectroscopic studies of $LaPO_4$: Ce/ Tb@$LaPO_4$@SiO_2 nanorods: Synthesis and role of surface coating. Vib. Spectrosc. 94: 43-48.

Badger, R.M. and Bauer, S.H. (1937). Spectroscopic studies of the hydrogen bond. II. The shift of the O– H vibrational frequency in the formation of the hydrogen bond. J. Chem. Phys. 5: 839-851.

Boontima, S. (2010). Vibrational spectroscopic study and thermal decomposition kinetics of some single and binary metal phosphate hydrates. Master of Science Thesis in Physical Chemistry, Graduate School. Khon Kaen University. Khon Kaen.

Buanam-Om, C. (1981). Raman and infrared spectroscopy of the structure of water (H_2O, HOD, D_2O) in stoichiometric crystalline hydrates and in electrolyte solutions. Dissertation, Philipps University of Marburg. Mauerberger. Marburg. Germany.

Cahil, A., Najdoski, M. and Stefov, V. (2007). Infrared and Raman spectra of magnesium ammonium phosphate hexahydrate (struvite) and its isomorphous analogues. IV. FTIR spectra of protiated and partially deuterated nickelammonium phosphate hexahydrate and nickel potassium phosphate hexahydrate. J. Mol. Struct. 834–836: 408–413.

Cahil, A., Šoptrajanov, B., Najdoski, M., Lutz, H.D., Engelen, B. and Stefov, V. (2008). Infrared and Raman spectra of magnesium ammonium phosphate hexahydrate

(struvite) and its isomorphous analogues. Part VI: FT-IR spectra of isomorphously isolated species. NH_4^+ ions isolated in $MKPO_4 \cdot 6H_2O$ (M = Mg; Ni) and PO_4^{3-} ions isolated in $MgNH_4AsO_4 \cdot 6H_2O$. J. Mol. Struct. 876: 255–259.

Chan, T.S., Liu, R.S. and Baginskiy, I. (2008). Synthesis, crystal structure, and luminescence properties of a novel green-yellow emitting phosphor $LiZn_{1-x}PO_4$: Mn_x for light emitting diodes. Chem. Mater. 20: 1215-1217.

Chan, T.S., Liu, R.S., Baginskiy, I., Bagkar, N. and Cheng, B.M. (2008). Vacuum Ultraviolet Excitable Mn^{2+} - Doped $LiZnPO_4$ Phosphors for PDP Applications. J. Electrochem. Soc. 155: J284-J286.

Chen, J., Vacchio, M.J., Wang, S., Chernova, N., Zavalij, P.Y. and Whittingham, M.S. (2008). The hydrothermal synthesis and characterization of olivines and related compounds for electrochemical applications. Solid State Ionics 178: 1676-1693.

Chen, Z., Chai, Q., Liao, S., He, Y., Wu, W. and Li, B. (2012). Preparation of $LiZnPO_4 \cdot H_2O$ via a novel modified method and its non-isothermal kinetics and thermodynamics of thermal decomposition. J. Therm. Anal. Calorim. 108: 1235-1242.

Danvirutai, C. and Jeradipalang, C. (1984). Presented in 10th Conference on Science and Technology of Thailand. Chiang Mai University. Chiang Mai, Thailand.

Dhevi, D.M., Prabu, A.A. and Kim, K.J. (2018). Infrared spectroscopic studies on crystalline phase transition of PVDF and PVDF/ hyperbranched polyester blend ultrathin films. Vib. Spectrosc. 94: 74-82.

Falk, M. and Knop, O. (1973). Water: A Comprehensive Treatise. New York: Plenum Press.

Fan, J., Yu, Y., Wang, Y., Wu, Q.H., Zheng, M. and Dong, Q. (2016). Nonaqueous synthesis of nano-sized $LiMnPO_4$/C as a cathode material for high performance lithium ion batteries. Electrochim. Acta 194: 52-58.

Feng, P.Y., Bu, X.H., Tolber, S.H. and Stucky, G.D. (1997). Syntheses and characterizations of chiral tetrahedral cobalt phosphates with zeolite ABW and related frameworks. J. Am. Chem. Soc. 119: 2497-2504.

Ferraro, J.R. and Ziomek, J.S. (1975). Introductory group theory and applications to molecular structure. 2nd ed. New York: Plenum Press.

Frost, R.L., Jagannadha Reddy, B., Martens, W.N. and Weier, M. (2006). The molecular structure of the phosphate mineral turquoise — a Raman spectroscopic study. J. Mol. Struct. 788: 224–231.

Frost, R.L. and Xi, Y.F. (2012). A vibrational spectroscopic study of the phosphate mineral Wardite $NaAl_3(PO_4)_2(OH)_4 \cdot 2(H_2O)$. Spectrochim. Acta Part A 93: 155– 163.

Frost, R.L., Xi, Y.F. and Scholz, R. (2013). A vibrational spectroscopic study of the phosphate mineral cyrilovite $Na(Fe^{3+})_3(PO_4)_2(OH)_4 \cdot 2(H_2O)$ and in comparison with wardite. Spectrochim. Acta Part A 108: 244–250.

Frost, R.L., Xi, Y.F., Scholz, R., Belotti, F.M. and Menezes Filho, L.A.D. (2013). A vibrational spectroscopic study of the phosphate mineral zanazziite – $Ca_2(MgFe^{2+})(MgFe^{2+}Al)_4Be_4(PO_4)_6 \cdot 6(H_2O)$. Spectrochim. Acta Part A 104: 250–256.

Frost, R.L., Xi, Y.F., Scholz, R., Lópeza, A. and Belotti, F.M. (2013). Vibrational spectroscopic characterization of the phosphate mineral hureaulite – $(Mn, Fe)_5(PO_4)_2(HPO_4)_2 \cdot 4(H_2O)$. Vib. Spectrosc. 66: 69–75.

Frost, R.L., Xi, Y.F., Scholz, R., Belotti, F.M. and Filho, M.C. (2013). The phosphate mineral sigloite $Fe^{3+}Al_2(PO_4)_2(OH)_3 \cdot 7(H_2O)$, An exception to the paragenesis rule – A vibrational spectroscopic study. J. Mol. Struct. 1033: 258–264.

Frost, R.L., Lopez, A., Xi, Y.F., Murta, N. and Scholz, R. (2013). The molecular structure of the phosphate mineral senegalite $Al_2(PO_4)(OH)_3 \cdot 3H_2O$ – A vibrational spectroscopic study. J. Mol. Struct. 1048: 420–425.

Frost, R.L., Xi, Y.F., Scholz, R. and de Brito Ribeiro, C.A. (2013). The molecular structure of the phosphate mineral chalcosiderite – A vibrational spectroscopic study. Spectrochim. Acta Part A 111: 24–30.

Halford, R.S. (1946). Motions of Molecules in Condensed Systems: I. Selection Rules, Relative Intensities, and Orientation Effects for Raman and Infra-Red Spectra. J. Chem. Phys. 14: 8-15.

Harrison, W.T.A., Gier, T.E., Nocol, J.M. and G.D. Stucky, (1995). Tetrahedral-framework lithium zinc phosphate phases: location of light-atom positions in $LiZnPO_4 \cdot H_2O$ by powder neutron diffraction and structure

determination of $LiZnPO_4$ by ab initio methods. J. Solid State Chem. 114: 249-257.

Horning, D.F. (1948). The Vibrational Spectra of Molecules and Complex Ions in Crystals. I. General Theory. J. Chem. Phys. 16: 1063-1076.

Izmailova, S.G., Vasiljeva, E.A., Karetina, I.V., Feoktistova, N.N. and Khvoshchev, S.S. (1996). Adsorption of methanol, ammonia and water on the zeolite-like alumino-phosphates $AlPO_4$-5, $AlPO_4$-17, and $AlPO_4$-18. J. Colloid Interface Sci. 179: 374–379.

Jensen, T.R. (1998). A new polymorph of $LiZnPO_4 \cdot H_2O$; synthesis, crystal structure and thermal transformation. J. Chem. Soc. Dalton Trans. 2261-2206.

Kim, D.H., Jeong, E.D., Kim, S.P. and Shim, Y.B. (2000). Effect of pH on the synthesis of $LiCoO_2$ with malonic acid and its charge/discharge behavior for a lithium secondary battery. Bull. Korean Chem. Soc. 21: 1125-1132.

Kullayakool, S., Danvirutai, C., Siriwong, K. and Noisong, P. (2013). Thermal behavior, surface properties and vibrational spectroscopic studies of the synthesized $Co_{3x}Ni_{3-3x}(PO_4)_2 \cdot 8H_2O$ ($0 \leq x \leq 1$). Solid State Sci. 24: 147-153.

Li, M.J., Wu, Z.L., Ma, Z., Schwartz, V., Mullins, D.R., Dai, S. and Overbury, S.H. (2009). CO oxidation on Au/$FePO_4$ catalyst: Reaction pathways and nature of Au sites. J. Catal. 266: 98–105.

Liao, S., Chen, Z.P., Tian, X.Z. and Wu, W.W. (2009). Synthesis and regulation of α- $LiZnPO_4 \cdot H_2O$ via a solid-state reaction at low-heating temperatures. Mater. Res. Bull. 44: 1428.-1431.

Liu, A., Liu, Y., Hu, Z., Gao, G., Xu, Y. and Lei, L. (2011). Electrochemical performance of $LiFePO_4$/C synthesized by solid state reaction using different lithium and iron sources. J. Phys. Chem. of Solids 72: 831-835.

Luck, W.A.P. (1976). The angle dependence of hydrogen bonding interaction in hydrogen bond. Amsterdam: North-Holland Publishers.

Ma, F., Zhang, X., He, P., Zhang, X., Wang, P. and Zhou, H. (2017). Synthesis of hierarchical and bridging carbon-coated $LiMn_{0.9}Fe_{0.1}PO_4$ nanostructure as cathode material with improved performance for lithium ion batteries. J. Power Sources 359: 408-414.

Mahmood, T., Nawaz, H., Ditta, A., Majeed, M.I., Hanif, M.A., Rashid, N., Bhatti, H.N., Nargis, H.F., Saleem. M., Bonnier, F. and Byrne, H.J. (2018). Raman spectral analysis for rapid screening of dengue infection. Spectrochim. Acta A 200: 136-142.

Mustafa, S., Murtaza, S., Naeem, A. and Farina, K. (2005). Sorption of divalent metal ions on $CrPO_4$. J. Colloid Interface Sci. 283: 287–293.

Noisong, P. and Danvirutai, C. (2010). A new synthetic route, characterization and vibrational studies of manganese hypophosphite monohydrate at ambient temperature. Spectrochim. Acta Part A 77: 890–894.

Novak, A. (1974). Hydrogen bonding in solids correlation of spectroscopic and crystallographic data. Struct. Bonding 18: 177-216.

Pejov, Lj., Šoptrajanov, B. and Jovanovski, G. (2000). Very low HOH bending frequencies. II. Quantum chemical study of the water bending potential in compounds of $MKPO_4 \cdot H_2O$ type. J. Mol. Struct. 563-563: 321-327.

Purcell, K.F. and Drago, R.S. (1967). Theoretical aspects of the linear enthalpy wavenumber shift relation for hydrogen-bonded phenols. J. Am. Chem. Soc. 89: 2874-2879.

Rao, C.N.R., Dwivedi, P.C., Ratajczak, H. and Thomas-Orville, W.J. (1975). Relation between O—H stretching frequency and hydrogen bond energy: re-examination of the Badger–Bauer rule. J. Chem. Soc., Faraday Trans. II. 71: 955-966.

Scherer, J.R. (1978). The vibrational spectroscopy of water, *In* Advances in Infrared and Raman spectroscopy. Clark R.J.H. and Hester, R.E. (Eds.) Philadelphia: Heyden. 5: 149-216.

Šoptrajanov, B. (2000). Very low H–O–H bending frequencies. I. Overview and infrared spectra of $NiKPO_4 \cdot H_2O$ and its deuterated analogues. J. Mol. Struct. 555: 21–30.

Šoptrajanov, B., Jovanovski, G. and Pejov, Lj. (2002). Very low H–O–H bending frequencies. III. Fourier transform infrared study of cobalt potassium phosphate monohydrate and manganese potassium phosphate monohydrate. J. Mol. Struct. 613: 47–54.

Šoptrajanov, B., Stefov, V., Kuzmanovski, I., Jovanovski, G., Lutz, H.D. and Engelen, B. (2002). Very low H–O–H bending frequencies. IV. Fourier transform infrared spectra of synthetic dittmarite. J. Mol. Struct. 613: 7–14.

Šoptrajanov, B., Stefov, V., Lutz, H.D. and Engelen, B. (2004). Infrared and Raman spectra of magnesium ammonium

phosphate hexahydrate (struvite) and its isomorphous analogues. II. The O– H/ N– H stretching region, *In* Spectroscopy of Emerging Materials. Kluwer Academic Pulishers. pp. 299-308.

Šoptrajanov, B., Cahil, A., Najdoski, M., Koleva, V. and Stefov, V. (2011). Infrared and Raman spectra of magnesium ammonium phosphate hexahydrate (struvite) and its isomorphous analogues. VIII. Spectra of protiated and partially deuterated magnesium rubidium phosphate hexahydrate and magnesium thallium phosphate hexahydrate. Acta Chim. Slov. 58: 478–484.

Sronsri, C., Noisong, P. and Danvirutai, C. (2016). Synthesis, characterization and vibrational spectroscopic study of Co, Mg co-doped $LiMnPO_4$. Spectrochim. Acta Part A 153: 436-444.

Stefov, V., Šoptrajanov, B., Spirovski, F., Kuzmanovski, I., Lutz, H.D. and Engelen, B. (2004). Infrared and Raman spectra of magnesium ammonium phosphate hexahydrate (struvite) and its isomorphous analogues. I. Spectra of protiated and partially deuterated magnesium potassium phosphate hexahydrate. J. Mol. Struct. 689: 1–10.

Stefov, V., Šoptrajanov, B., Kuzmanovski, I., Lutz, H. D. and Engelen, B. (2005). Infrared and Raman spectra of magnesium ammonium phosphate hexahydrate (struvite) and its isomorphous analogues. III. Spectra of protiated and partially deuterated magnesium ammonium phosphate hexahydrate. J. Mol. Struct. 752: 60–67.

Stefov, V., Šoptrajanov, B., Najdoski, M., Engelen, B. and Lutz, H.D. (2008). Infrared and Raman spectra of magnesium ammonium phosphate hexahydrate (struvite) and its isomorphous analogues. V. Spectra of protiated and partially deuterated magnesium ammonium arsenate hexahydrate (arsenstruvite). J. Mol. Struct. 872: 87–92.

Stefov, V., Cahil, A., Šoptrajanov, B., Najdoski, M., Spirovski, F., Engelen, B., Lutz, H.D. and Koleva, V. (2009). Infrared and Raman spectra of magnesium ammonium phosphate hexahydrate (struvite) and its isomorphous analogues. VII: Spectra of protiated and partially deuterated hexagonal magnesium caesium phosphate hexahydrate. J. Mol. Struct. 924–926: 100–106.

Stefov, V., Abdija, Z., Najdoski, M., Koleva, V., Petruševski, V.M., Runčevski, T., Dinnebier, R.E. and Šoptrajanov, B. (2013). Infrared and Raman spectra of magnesium ammonium phosphate hexahydrate (struvite) and its isomorphous analogues. IX. Spectra of protiated and partially deuterated cubic magnesium caesium phosphate hexahydrate. Vib. Spectrosc. 68: 122-128.

Xu, L., Wang, S., Zhang, X., He, T., Lu, F., Li, H. and Ye, J. (2018). A facile method of preparing $LiMnPO_4$/ C reduced graphene oxide aerogel as cathodic material for aqueous, lithium-ion hybrid super capacitors. Appl. Surface Sci. 428: 977-985.

❑❑❑❑❑